

EVOLUTIONARY CONSEQUENCES OF DUSTY TORI IN ACTIVE GALACTIC NUCLEI

JIAN-MIN WANG¹, EN-PENG ZHANG^{1,2} AND BIN LUO^{1,2}
 Received 2004 September 2; accepted 2005, May 18

ABSTRACT

Deep surveys of *Chandra* and *HST* (Hubble Space Telescope) show that active galactic nucleus (AGN) populations are changing with hard X-ray luminosities. This arises an interesting question whether the dusty torus is evolving with the central engines. We assemble a sample of 50 radio-quiet PG quasars to tackle this problem. The covering factors of the dusty tori can be estimated from the multiwavelength continuum. We find they are strongly correlated with the hard X-ray luminosity. Interestingly this correlation agrees with the fraction of type II AGNs discovered by *Chandra* and *HST*, implying strong evidence for that the AGN population changing results from the evolution of the tori. We also find that the frequencies of the dips around $1\mu\text{m}$ in the continuum correlate with the covering factors in the present sample, indicating the dip frequencies are adjusted by the covering factors. In the scenario of fueling black hole from the torus, the covering factor is a good and the dip frequency is a potential indicator of the torus evolution.

Subject headings: galaxies: active – galaxies: nuclei

1. INTRODUCTION

The polarized spectrum of NGC 1068 shows a broad $H\beta$ feature indicating the presence of a hidden active nucleus by a geometrically and optically thick torus (Antonucci & Miller 1985). The opening angle is estimated about $74^\circ \sim 96^\circ$ for Seyfert sample from the relative number of type II AGNs (e.g. Osterbrock & Shaw 1988; Tovmassian 2001), similar to PG quasars from continuum (Cao 2005). The unification scheme is successful in explanation of the Seyfert 1/2 dichotomy (Antonucci 1993). However the strong unification scheme, namely a torus with a constant H/R , seems difficult in explanation of the multi-wavelength continuum (e.g. Wilkes et al. 1999). Deep surveys of *Chandra* and *HST* show the fraction (P_{II}) of type II AGNs decreases with 2-10keV luminosities (L_X) (Ueda et al. 2003; Steffen et al. 2003; Hasinger 2004, hereafter H04; but see a different explanation in Zhang 2005). An selection effect in the $P_{\text{II}} - L_X$ relation has been argued by Treister et al. (2004) based on continuum of Great Observatories Origin Deep Survey, but the highly spectroscopically complete deep and wide-area *Chandra* surveys support this relation (Barger et al. 2005, hereafter B05). This controversial issue motivates us to explore whether there is a relation between the obscuring matter and AGN's engines.

The infrared emission may provide new clues to look into the properties of the covering area. Infrared Space Observatory (*ISO*) data show that near- to mid-IR SEDs in PG quasars are likely due to reprocessing of dust heated by the central AGNs, even far IR band (Haas et al. 2000, 2003). Radio-quiet PG quasars usually have prominent big blue bumps (Elvis et al. 1994) and hence they tend to have small inclinations to observers (Laor 1990). This is also supported by the low $E_{\text{B}-\text{V}}$ absorption and non-spherical distribution of dust (Haas et al. 2000). The differences among these objects can be neglected in anisotropic properties of infrared (from compact tori) and optical ultraviolet emissions (from accretion disks). This allows us to reliably get the properties of torus obscuration and then to find evolutionary consequences of the tori from the multi-wavelength continuum.

In this Letter, we investigate the covering factors of the tori from the multi-wavelength continuum. We show evidence for the agreement between the covering factors and the population fractions of AGNs. This implies that the AGN populations are changing with the evolution of the opening angle of the tori.

2. THE SAMPLE

Following Granato & Danese (1994), we define

$$\mathcal{R} = \frac{\int_{\text{IR}} L_\nu d\nu}{\int_{\text{OUV}} L_\nu d\nu}, \quad (1)$$

where L_ν is the continuum of the quasar, "IR" and "OUV" stand for the integral limits of the spectrum in infrared and optical-ultraviolet ($0.01 - 1\mu\text{m}$) bands, respectively. Since the uncertainties of extreme ultraviolet (EUV) spectrum, we get the EUV luminosity $L_{\text{EUV}}(0.01 - 0.1\mu) \approx 2.2L_{0.1-1\mu}$ by simply extrapolating the spectrum of $F_\nu \propto \nu^{-0.5}$ (Rowan-Robinson 1995), where $L_{0.1-1\mu}$ is the luminosity integrated from 0.1 to $1\mu\text{m}$ and can be conveniently obtained from the observations. EUV luminosity has uncertainties less than 20% from this extrapolation (Granato & Danese 1994). We thus have $L_{\text{OUV}} \approx 3.2L_{0.1-1\mu}$, with uncertainties less than $\sim 14\%$ due to EUV. Considering the debate of the IR origin from AGNs (e.g. Rowan-Robinson 1995; Haas et al. 2003), we use three bins as the main contribution from the torus: $L_{1-25\mu}$, $L_{1-60\mu}$ and $L_{1-100\mu}$, which are luminosities integrated for $1 - 25\mu\text{m}$, $1 - 60\mu\text{m}$ and $1 - 100\mu\text{m}$, respectively, and have \mathcal{R}_{25} , \mathcal{R}_{60} and \mathcal{R}_{100} subsequently. We searched for radio-quiet PG quasars with 2 - 10 keV X-ray and IR observations from the published literatures, but we exclude some quasars based on the below criterion. The available data of infrared spectrum are from *IRAS* and *ISO* observations. The sample is given in Table 1. The observed flux density is converted to monochromatic luminosity in the rest frame using $H_0 = 75 \text{ km s}^{-1} \text{ Mpc}^{-1}$ and $q_0 = 0.5$.

We get the dip frequency via fitting the optical-ultraviolet spectrum as a power law and the near infrared spectrum (shorter than $5\mu\text{m}$) as the Planck function (Barvainis 1990, Kobayashi

¹ Laboratory for High Energy Astrophysics, Institute of High Energy Physics, Chinese Academy of Sciences, Beijing 100039, P. R. China, wangjm@mail.ihep.ac.cn

² Graduate School of Chinese Academy of Sciences, Beijing 100039, P. R. China

TABLE 1. THE PG QUASAR SAMPLE (SEE THE COMPLETE TABLE IN ELECTRONIC VERSION)

Name	z	$\log L_{1-25\mu}$	$\log L_{1-60\mu}$	$\log L_{1-100\mu}$	$\log L_{0.1-1\mu}$	$\log \nu_{\text{dip}}$	$\log L_X$	Ref.
(1)	(2)	(3)	(4)	(5)	(6)	(7)	(8)	(9)
PG0003+199	0.026	44.51 ± 0.03	44.57 ± 0.04	< 44.59	44.59 ± 0.03	14.50 ± 0.09	43.06 ± 0.02	11, 12, 4
PG0026+129	0.142	< 45.17	< 45.33	< 45.37	45.37 ± 0.04	14.39 ± 0.10	44.43 ± 0.07	2, 12, 12

et al. 1993). When the parameter χ^2 defined as

$$\chi^2 = \sum_i^N [f_1 \nu_i^{-\alpha} + f_2 B(\nu_i, T_{\text{evap}}) - f_{\nu_i}^0]^2, \quad (2)$$

reaches a minimum value, we get the best-fitted spectrum $f_\nu = f_1 \nu^{-\alpha} + f_2 B(\nu, T_{\text{evap}})$ and hence the dip frequency of the spectrum around $1\mu\text{m}$. Here T_{evap} is the evaporation temperature of dust, $B(\nu_i, T_{\text{evap}})$ is the Planck function and $f_{\nu_i}^0$ is the flux at a frequency ν_i . We take the evaporation temperature of dust $T_{\text{evap}} = 1500\text{K}$. The error bar of the dip frequency is then given by $\sigma_{\nu_{\text{dip}}}^2 = (\partial \nu_{\text{dip}} / \partial f_1)^2 \sigma_{f_1}^2 + (\partial \nu_{\text{dip}} / \partial f_2)^2 \sigma_{f_2}^2 + (\partial \nu_{\text{dip}} / \partial \alpha)^2 \sigma_\alpha^2$, where σ_{f_1} , σ_{f_2} and σ_α are the error bars of f_1 , f_2 and α deduced from uncertainties of $f_{\nu_i}^0$. The quality of the spectra of some objects around the dips is not good enough to obtain the dip frequency in the present sample. We exclude those objects with $\Delta \log \nu_{\text{dip}} \geq 0.2$ and get the exact frequencies of the dips in 34 quasars given in Tab 1.

We should note that the near IR emission from host galaxies may have potential influence on the ratio of \mathcal{R} if the hosts are bright enough. A crude criterion for the host contribution is the ratio of luminosities of quasar to host at R - or V -band from the available data. It can be obtained by extrapolating the OUV spectrum to 1μ and getting H -band luminosity of the quasar from its mean NIR spectrum of $f_\nu \propto \nu^{-1.3}$ (Haas et al. 2003) and H -band luminosity of host from M_V or M_R based on the spectrum of star light (Kriss 1988). We have the critical ratios of luminosities of quasars to hosts $L_V^Q / L_V^H \geq 3.4$ at V -band and $L_R^Q / L_R^H \geq 2.4$ at R -band, which correspond to $L_H^Q \geq 2L_H^H$ at H -band. Here the upper scripts Q and H refer to quasars and hosts. Though we exclude some quasars by the criteria, we have to keep in mind that the present sample could potentially cover other quasars (we are not able to distinguish them without available data of their host galaxies). With these criteria, the uncertainties of the covering factors are $\Delta C_0 / C_0 \leq 0.05$ and $\Delta C_1 / C_1 \leq 0.07$ and the uncertainties of the dip frequencies are $\Delta \log \nu_{\text{dip}} \leq 0.03$ due to the host's contaminations. It should also be noted that the optical component extends past $1\mu\text{m}$ to slightly contribute to IR flux, which is neglected in this paper. We also note that the apertures are different for each bands (see Table 1). Neugebauer et al. (1987) calibrated $1.3 - 10.1\mu\text{m}$ photometry with respect to the standard stars. Haas et al. (2000; 2003) corrected the source flux for the aperture size. We should use the total IR emission from the torus to determine the covering factor, however, the far IR emission and some of mid-IR in some AGNs could be powered by the extended torus, the narrow line region (e.g. NGC 1068; Bock et al. 2000), starburst or star from galactic stars. It is difficult to estimate the cutoff wavelength of the infrared emission from the torus, but three ratios of \mathcal{R}_{25} , \mathcal{R}_{60} and \mathcal{R}_{100} are used to show how the covering factor relies on the cutoff wavelength. A crude estimation of the distance of dust to the center engine shows $R \leq 4.7L_{45}^{1/2} \lambda_{25}^2$ pc from $aT^4 \leq L/4\pi R^2 c$, where $L_{45} = L/10^{45} \text{erg s}^{-1}$, $\lambda_{25} = \lambda/25\mu$, a and c are the black body radiation constant and the light speed, respectively, based on the

assumption that the dust is heated by the central engine. Thus the ratios of \mathcal{R}_{25} , \mathcal{R}_{60} and \mathcal{R}_{100} correspond to the distances of dust, $4.7L_{45}^{1/2} \lambda_{25}^2$, $27.1L_{45}^{1/2} \lambda_{60}^2$ and $75.2L_{45}^{1/2} \lambda_{100}^2$ pc, respectively, where $\lambda_{60} = \lambda/60\mu$, $\lambda_{100} = \lambda/100\mu$.

3. GEOMETRY OF TORUS AND STATISTICS

3.1. Covering factors and AGN populations

The geometry and physical conditions (e.g. dust and cloud properties) of the torus are not fully understood. Emergent spectra from the tori have been extensively calculated for different geometry by Granato & Danese (1994) and Efstathiou & Rowan-Robinson (1995) stemming from the work of Pier & Krolik (1992) and are able to generally fit the observed IR continuum. However, the IR optically thin grains can also produce the observed IR spectra of PG quasars (Barvainis 1990). This assumption is partially supported by the recent observations of NGC 1068 of Jaffe et al. (2004), who find a spatially averaged peak silicate absorption depth, $\langle \tau_{\text{SiO}} \rangle = 0.3$ and $\langle \tau_{\text{SiO}} \rangle = 2.1$ in front of the $T = 320\text{K}$ and the hot components, respectively. A clumpy model of torus has been proposed by Nenkova et al. (2002) and also gives reasonable infrared SEDs. Though these uncertainties, the continuum may allow us to estimate the covering factors.

Assuming the isotropic emission from the central engine, Granato & Danese (1994) give the covering factor obtained from \mathcal{R} based on the energy balance

$$C = \frac{\mathcal{R}}{1 + \mathcal{R}(1-p)} = \begin{cases} C_0 = \frac{\mathcal{R}}{1+\mathcal{R}} & (p=0), \\ C_1 = \mathcal{R} & (p=1), \end{cases} \quad (3)$$

where p is the ratio between the integrated flux emitted by the dust at the equator and that emitted at the pole. For $p = 1$, the torus is essentially transparent to infrared radiation, whereas the $p = 0$ torus is optically thick to infrared photons. Though the emission from accretion disks is anisotropic (Netzer 1985), it is treated as a point of the illuminating energy source in the popular models (Pier & Krolik 1992; Granato & Danese 1994; Efstathiou & Rowan-Robinson 1995). The differences due to orientations could be neglected in the observed optical, ultraviolet and infrared luminosities among the objects in the present PG quasar sample. Furthermore, it may be reasonable to assume that the torus and disk are co-plane, implying the orientation effects of disk and torus are similar. The parameter \mathcal{R} thus only weakly depends on the orientations.

We use the ASURV (Isobe et al. 1986) to analyze the correlation for the censored data of the present sample. The results are given in Table 2, which are shown in Fig 1a and 1b. We find that $C-L_X$ for \mathcal{R}_{25} is much stronger than that for \mathcal{R}_{60} and \mathcal{R}_{100} , especially C_1-L_X for \mathcal{R}_{25} nicely agrees with the fraction of type II AGNs (see below). The scatterers in this plot may be caused by the complex geometry of the real torus and different values of p in each quasars. We have checked whether the $\mathcal{R}/C-L_X$ correlation is introduced by that of L_X and L_{OUV} . Using the multivariate correlation

TABLE 2. THE CORRELATION ANALYSIS

	$\mathcal{C}_0 - L_X$				$\mathcal{C}_1 - L_X$			
	q	k	ρ	p	q	k	ρ	p
\mathcal{R}_{25}	-0.36 ± 0.07	-0.17 ± 0.04	-0.53	3.0×10^{-4}	-0.16 ± 0.10	-0.22 ± 0.05	-0.53	3.0×10^{-4}
\mathcal{R}_{25}^a	-0.41 ± 0.07	-0.12 ± 0.04	-0.51^b	1.7×10^{-3}	-0.22 ± 0.09	-0.16 ± 0.05	-0.50^b	2.0×10^{-3}
\mathcal{R}_{60}	-0.42 ± 0.08	-0.10 ± 0.04	-0.33	2.4×10^{-2}	-0.21 ± 0.12	-0.13 ± 0.08	-0.33	2.4×10^{-2}
\mathcal{R}_{100}	-0.32 ± 0.09	-0.13 ± 0.05	-0.36	1.3×10^{-2}	-0.08 ± 0.14	-0.19 ± 0.07	-0.36	1.3×10^{-2}

NOTES. $\log C = k \log L_{X,42} + q$, where $L_{X,42} = L_X / 10^{42} \text{ erg s}^{-1}$. ρ is the Spearman's coefficient and p is the null-probability. *a*: the case excluding the upper limit sources. *b*: refers to the Pearson's coefficient. There are too many upper limit sources in \mathcal{R}_{60} and \mathcal{R}_{100} . It should be noted the ASURV program using survival statistics for the upper limits assumes that the limits are distributed like the detections.

analysis, we find a strong correlation among $L_{1-25\mu}$, L_X and L_{OUV} as $\log L_{1-25\mu} = 6.53 + 0.98 \log L_{\text{OUV}} - 0.14 \log L_X$ with a Pearson's coefficient of $r = 0.98$, which can be translated into $\log \mathcal{R}_{25} = 6.53 - 0.02 \log L_{\text{OUV}} - 0.14 \log L_X$. This is consistent with the $\mathcal{C} - L_X$ for \mathcal{R}_{25} in Table 2. Thus the $\mathcal{C} - L_X$ relations here are true. It is interesting to note the dependence of the correlation coefficients for $\mathcal{C} - L_X$ vs \mathcal{R} for various IR cutoffs. This might imply a constraint on the extent to which the FIR is heated by AGN.

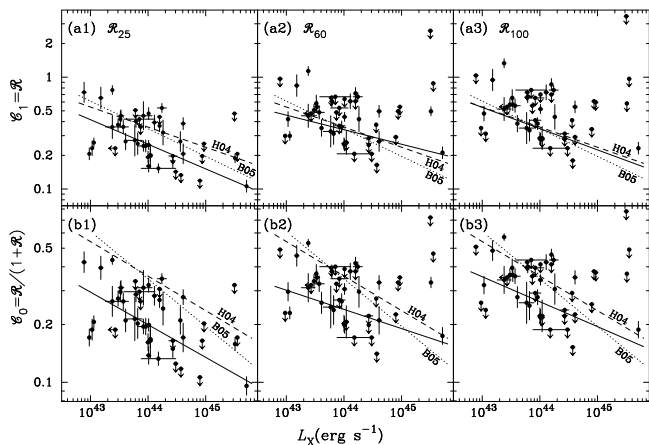


FIG. 1.— The plot of $\mathcal{C} - L_X$. The solid line represents the best fit of the correlation by the least square method. It is found that $\mathcal{C}_1 - L_X$ relation for \mathcal{R}_{25} is consistent with $P_{\text{II}} - L_X$ relation found by *Chandra* and *HST* deep surveys. The dashed and dotted lines are the fitted results from the surveys in Hasinger (2004) and Barger et al. (2005), respectively.

With the geometry of the torus in Granato & Danese (1994), we have $\Delta\Omega/4\pi = \cos\theta = \mathcal{C}$, where $\Delta\Omega$ is the solid angle of the torus subtending the accretion disk and θ is the half opening angle ($\leq 90^\circ$). The deep surveys of *HST* and *Chandra* provide the fraction of type II AGNs, $P_{\text{II}} = N_2/(N_1 + N_2)$, where N_1 and N_2 are the numbers of type I and II AGNs, respectively. If the observer is located within the opening cone of the dusty torus, the object appears as type I, otherwise as type II. We thus have $P_{\text{II}} = \Delta\Omega/4\pi$ allowing for the comparison with the results from surveys. The available data can be found in H04, who summarizes the results from *Chandra*, *HST* and *ASCA* (Ueda et al. 2003) based on the criterion of hydrogen column density. There are some type II AGNs missed in X-ray band, the $P_{\text{II}} - L_X$ relation may be caused by the selection effect (Treister et al. 2004). In addition, some of AGNs in the deep *Chandra* field show some elusive properties in optical band (Maiolino et al. 2003), but a highly spectroscopic research on the populations of *Chandra* deep field shows a robust $P_{\text{II}} - L_X$ relation (B05). We fit the data in Fig 6 in H04 and Fig 19 in B05 using

the least square method and get,

$$\log P_{\text{II}} = \begin{cases} (-0.18 \pm 0.02) + (-0.09 \pm 0.01) \log L_{X,42} & \text{(H04),} \\ (0.03 \pm 0.50) + (-0.24 \pm 0.34) \log L_{X,42} & \text{(B05).} \end{cases} \quad (4)$$

It is very interesting to find the $P_{\text{II}} - L_X$ relations in H04 and B05 nicely agree with each other within the uncertainties. This reflects some physical connections between the obscuring X-ray and the emission line regions in AGNs. Comparing eq. (4) with Table 2, we find that the present $\mathcal{C}_1 - L_X$ relation for \mathcal{R}_{25} is in agreement with the results of H04 and B05.

The agreement between the $\mathcal{C}_1 - L_X$ for \mathcal{R}_{25} and the $P_{\text{II}} - L_X$ relations indicates: 1) a natural connection between the reprocessing matter (the compact torus) and the obscuring X-ray parts of AGNs (H04) as well as the optical emission line region (B05); 2) the dusty torus evolution results in the population changing of AGNs; 3) the $\mathcal{C}_1 - L_X$ and $P_{\text{II}} - L_X$ relations are intrinsic and thus greatly enhances the unification scheme of compact torus for AGNs, especially the $\mathcal{C}_1 - L_X$ for \mathcal{R}_{60} and \mathcal{R}_{100} are much scattered and significantly deviate from the relation H04 and B05. The present sample is different from that in H04 and B05, so the $\mathcal{C}_1 - L_X$ for \mathcal{R}_{25} just strengthens the intrinsically physical connections of the torus evolution and population changing. It would be important if the $P_{\text{II}} - L_X$ relation can be confirmed for the *same* sample in different ways.

A self-regulation is set up between the sublimation of torus and the accretion process. A toy model of the torus fueling the black hole gives $\dot{M} \propto C^{-2}$, where \dot{M} is the accretion rate of the disk [see their eq. (9) and (15) in Krolik & Begelman (1988)]. We thus have a simple relation of $C \propto L_X^{-1/2}$ if $L_X \propto \dot{M}$. This theoretical prediction is much steeper than the observational results in this paper, but the trend of $\mathcal{C} - L_X$ relation agrees with eq. (4) and $\mathcal{C}_1 - L_X$ for \mathcal{R}_{25} . A proper explanation of the $\mathcal{C}_1 - L_X$ relation will depend on detail micro-physics of the torus and is beyond the scope of this Letter. The evolution of the torus geometry could be controlled by the collisions among clouds inside the torus (Krolik & Begelman 1988), which inevitably lead to detectable emissions in radio and sub-GeV bands (Wang 2004). In addition, the X-ray Baldwin effect of the iron narrow $K\alpha$ line can be derived from the changing population of type II AGNs based on the deep surveys, strongly implying an evolutionary consequence of the tori (Zhou & Wang 2005).

3.2. dip frequencies

It is well known that the dip may be caused by dust evaporation and its frequency corresponds to the evaporation temperature (Sanders et al. 1989). The observed 1μ -dip frequency may depend on both the orientation of the torus and the covering factor, but we focus on how it relies on C . Fig 2a and 2b

show this dependence. Using the ASURV, we obtain

$$\log \nu_{\text{dip}} = \begin{cases} (14.55 \pm 0.04) + (0.14 \pm 0.07) \log C_0, \\ (14.52 \pm 0.03) + (0.11 \pm 0.05) \log C_1. \end{cases} \quad (5)$$

with Spearman's $\rho = 0.50$ and probability is 4.2×10^{-3} , and $\rho = 0.50$ and probability is 4.4×10^{-3} , respectively. The scatters in the plots may be caused mainly by the quality of the data, inclination differences among these objects, the complicated structures of the torus and potentially the contamination of host galaxies at $1\mu\text{m}$. However $\nu_{\text{dip}} - C$ relation still shows that the dip frequencies are adjusted by covering factors of the torus. It could be qualitatively explained by the changes of the covering factors of the torus due to AGN evolutions. ν_{dip} as a powerful probe of the covering factor could be robust in future for good quality data and detail calculations of the radiation transfer in the torus.

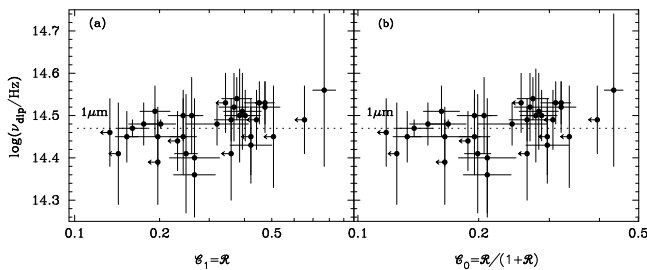


FIG. 2.— The covering factor C and the dip frequency ν_{dip} . This correlation shows an intrinsic connection between the torus and the accretion disk in AGNs, implying a fueling process to a black hole.

4. CONCLUSIONS AND DISCUSSIONS

Fueling the black hole will change the covering factor of the torus. It is thus expected that the covering factor could be a good indicator of the activity process of the black holes, showing the evolution of the active nucleus. Here we suggest an evolutionary sequence: higher $C \rightarrow$ lower C . We find two clues to understanding the evolution: 1) changing populations of type II AGNs as one consequence of AGN evolution due to increases of the opening angles; 2) the dip frequency increases with covering factor. The two consequences could be used to trace the active processes of galactic nuclei statistically.

The $\nu_{\text{dip}} - C$ relation provides a new clue to understand the relation between the accretion disks and the tori. It reflects the inter region between the outer boundary of the disks and the inner edge of the torus. We poorly understand the physical processes in this region as well as how to fuel the black hole on pc scale. Future observations of infrared interferometry telescopes could unveil something important taking place in this region, especially work on the survey sample would produce more robust results (Steffen et al. 2004). It is expected for *Spitzer* to make an attempt for a sample of deep surveys to construct more solid statistic properties of the tori.

The authors are grateful to the referee, R. Antonucci, for very helpful comments and constructive criticism improving the manuscript. S. N. Zhang is thanked for discussions. This research is supported by a Grant for Distinguished Young Scientists from NSFC-10325313, NSFC-10233030 and 973 project.

REFERENCES

- Antonucci, R. R. J., 1993, ARA&A, 31, 473
 Antonucci, R. R. J. & Miller, J. S., 1985, ApJ, 297, 621
 Barger, A. J., et al., 2005, AJ, 129, 578
 Barvainis, R., 1990, ApJ, 353, 419
 Bock, J. J., et al., 2000, AJ, 120, 2904
 Cao, X., 2005, ApJ, 619, 86
 Efsthathious, A. & Rowan-Robinson, M., 1995, MNRAS, 273, 649
 Elvis, M., et al. 1994, ApJS, 95, 1
 George, I. M., et al. 2000, ApJ, 531, 52
 Granato, G. L. & Danese, L., 1994, MNRAS, 268, 235
 Haas, M., et al. 2000, A&A, 354, 453
 Haas, M., et al. 2003, A&A, 402, 87
 Hasinger, G., 2004, Nucl. Phys. B (Proc Suppl.), 132, 86
 Isobe, T. Feigelson, E. D. & Nelson, P. L., 1986, ApJ, 306, 490
 Jaffe, W., et al., 2004, Nature, 429, 471
 Kobayashi, Y., et al., 1993, ApJ, 404, 94
 Kriss, G.A., 1988, ApJ, 324, 809
 Krolik, J.H. & Begelman, M.C., 1988, ApJ, 329, 702
 Laor, A., 1990, MNRAS, 246, 369
 Lawson, A. J., & Turner, M. J. L., 1997, MNRAS, 288, 92
 Maiolino, R., et al. 2003, MNRAS, 344, L59
 Nenkova, M., Ivezić, Z. & Elitzur, M., 2002, ApJ, 570, L9
 Netzer, H., 1985, MNRAS, 216, 63
 Neugebauer, G., et al., 1987, ApJS, 63, 615
 Osterbrock, D.E. & Shaw, R.A., 1988, ApJ, 327, 89
 Page, K. L., O'Brien, P. T. et al. 2004, MNRAS, 347, 316
 Piconcelli, E., et al., 2004, astro-ph/0411051
 Pier, E. A. & Krolik, J. H., 1992, ApJ, 401, 99
 Porquet, D., et al. 2004, A&A, 422, 85
 Reeves, J. N. & Turner M. J. L. 2000, MNRAS, 316, 234
 Sanders, D.B., et al., 1989, ApJ, 347, 29
 Steffen, A.T. et al., 2003, ApJ, 596, L23
 Steffen, A.T. et al., 2004, AJ, 128, 1483
 Tovmassian, H. M., 2001, Astron. Nachr. 2, 87
 Treister, E., et al., 2004, ApJ, 616, 123
 Ueda, Y., et al., 2003, ApJ, 598, 886
 Wang, J.-M., 2004, ApJ, 614, L21
 Wilkes, B. J., et al. 1999, ApJ, 513, 76
 Zhang, S. N., 2005, ApJ, 618, L79
 Zhou, X.-L. & Wang, J.-M., 2005, ApJ, 618, L83

Table 1. THE PG QUASAR SAMPLE

Name	z	$\log L_{1-25\mu}$	$\log L_{1-60\mu}$	$\log L_{1-100\mu}$	$\log L_{0.1-1\mu}$	$\log \nu_{\text{dip}}$	$\log L_X$	Ref.
(1)	(2)	(3)	(4)	(5)	(6)	(7)	(8)	(9)
PG0003+199	0.026	44.51 ± 0.03	44.57 ± 0.04	< 44.59	44.59 ± 0.03	14.50 ± 0.09	43.06 ± 0.02	11, 12, 4
PG0026+129	0.142	< 45.17	< 45.33	< 45.37	45.37 ± 0.04	14.39 ± 0.10	44.43 ± 0.07	2, 12, 12
PG0043+039	0.384	< 45.82	< 46.13	< 46.19	45.95 ± 0.03	14.44 ± 0.07	< 43.43	2, 3, 4
PG0049+171	0.064	< 44.45	< 44.65	< 44.71	$44.32^{+0.04}_{-0.03}$	14.45 ± 0.09	43.85 ± 0.27	1, 12, 12
PG0050+124	0.061	45.31 ± 0.03	45.48 ± 0.04	45.55 ± 0.04	44.92 ± 0.03	14.56 ± 0.18	43.38 ± 0.01	2, 12, 4
PG0052+251	0.155	45.22 ± 0.03	< 45.35	< 45.40	45.53 ± 0.03	14.45 ± 0.06	44.18 ± 0.30	2, 12, 12
PG0804+761	0.100	45.36 ± 0.04	45.48 ± 0.04	45.50 ± 0.04	$45.35^{+0.13}_{-0.12}$	14.48 ± 0.05	44.26 ± 0.01	1, 12, 4
PG0844+349	0.064	44.74 ± 0.03	44.83 ± 0.04	44.86 ± 0.04	$44.83^{+0.10}_{-0.11}$...	43.82 ± 0.01	12, 12, 6
PG0947+396	0.206	< 45.43	< 45.57	< 45.63	45.28 ± 0.04	14.49 ± 0.07	44.20 ± 0.04	11, 3, 7
PG0953+414	0.239	< 45.71	< 45.80	< 45.84	46.08 ± 0.04	14.46 ± 0.08	44.57 ± 0.04	11, 3, 7
PG1048+342	0.167	< 45.27	< 45.40	< 45.46	45.21 ± 0.04	14.41 ± 0.11	43.87 ± 0.04	11, 3, 7
PG1114+445	0.144	45.30 ± 0.03	< 45.43	< 45.47	45.12 ± 0.04	14.52 ± 0.06	44.01 ± 0.01	1, 3, 4
PG1115+407	0.154	< 45.19	< 45.30	< 45.35	44.98 ± 0.04	14.45 ± 0.12	43.78 ± 0.04	11, 3, 7
PG1115+080	1.718	< 47.37	< 48.11	< 48.24	47.19 ± 0.04	14.53 ± 0.05	45.50 ± 0.04	11, 3, 14
PG1116+215	0.177	45.66 ± 0.04	< 45.81	< 45.87	45.91 ± 0.04	14.48 ± 0.05	44.43 ± 0.01	1, 12, 4
PG1206+459	1.158	< 46.73	< 47.13	< 47.22	46.93 ± 0.04	...	44.94 ± 0.04	11, 3, 14
PG1211+143	0.085	45.22 ± 0.04	45.34 ± 0.04	45.38 ± 0.04	45.29 ± 0.07	14.36 ± 0.09	43.61 ± 0.01	1, 12, 4
PG1244+026	0.048	44.15 ± 0.04	44.41 ± 0.04	44.46 ± 0.04	$44.28^{+0.11}_{-0.06}$...	43.03 ± 0.01	1, 12, 4
PG1247+267	2.038	< 47.19	< 47.82	< 47.86	47.37 ± 0.04	...	45.55 ± 0.03	2, 3, 4
PG1307+085	0.155	< 45.09	< 45.25	< 45.30	$45.43^{+0.05}_{-0.06}$	14.41 ± 0.12	44.48 ± 0.04	2, 12, 12
PG1351+695	0.030	44.27 ± 0.04	44.37 ± 0.04	44.43 ± 0.04	$44.21^{+0.17}_{-0.11}$...	43.38 ± 0.12	11, 12, 12
PG1352+183	0.152	45.12 ± 0.04	< 45.30	< 45.35	45.23 ± 0.03	14.45 ± 0.09	43.92 ± 0.10	11, 12, 12
PG1402+261	0.164	45.39 ± 0.04	< 45.51	< 45.56	45.60 ± 0.04	14.51 ± 0.06	44.00 ± 0.04	1, 3, 7
PG1404+226	0.098	44.48 ± 0.04	< 44.64	< 44.71	44.66 ± 0.04	...	42.98 ± 0.02	1, 3, 4
PG1407+265	0.944	46.47 ± 0.03	46.89 ± 0.04	< 46.96	46.69 ± 0.03	...	45.51 ± 0.01	1, 12, 4
PG1411+442	0.089	45.11 ± 0.04	45.19 ± 0.04	45.21 ± 0.04	44.95 ± 0.04	14.53 ± 0.05	43.53 ± 0.05	2, 3, 4
PG1416-129	0.129	44.99 ± 0.04	< 45.14	< 45.18	$45.06^{+0.11}_{-0.09}$	14.40 ± 0.14	44.56 ± 0.01	1, 12, 4
PG1426+015	0.086	45.09 ± 0.04	45.21 ± 0.04	45.25 ± 0.04	$45.29^{+0.11}_{-0.16}$	14.45 ± 0.07	44.04 ± 0.04	1, 12, 6
PG1427+480	0.221	45.07 ± 0.04	45.26 ± 0.04	45.31 ± 0.04	45.36 ± 0.04	14.47 ± 0.12	44.01 ± 0.04	1, 3, 7
PG1440+356	0.077	45.01 ± 0.04	45.14 ± 0.04	45.19 ± 0.04	44.93 ± 0.04	14.54 ± 0.05	43.48 ± 0.01	1, 3, 4
PG1444+407	0.267	45.65 ± 0.04	45.82 ± 0.04	45.85 ± 0.04	45.76 ± 0.04	14.50 ± 0.06	43.96 ± 0.01	1, 3, 4

Table 1—Continued

Name	z	$\log L_{1-25\mu}$	$\log L_{1-60\mu}$	$\log L_{1-100\mu}$	$\log L_{0.1-1\mu}$	$\log \nu_{\text{dip}}$	$\log L_X$	Ref.
(1)	(2)	(3)	(4)	(5)	(6)	(7)	(8)	(9)
PG1501+106	0.036	44.50 ± 0.04	44.64 ± 0.04	44.69 ± 0.04	$44.37^{+0.09}_{-0.07}$	14.38 ± 0.09	43.52 ± 0.02	1, 12, 8
PG1543+489	0.400	45.95 ± 0.04	46.24 ± 0.04	46.32 ± 0.04	45.88 ± 0.04	14.52 ± 0.08	44.20 ± 0.02	1, 3, 4
PG1613+658	0.129	45.28 ± 0.04	45.47 ± 0.04	45.55 ± 0.04	$45.18^{+0.06}_{-0.10}$	14.51 ± 0.09	44.11 ± 0.04	2, 12, 6
PG1626+554	0.133	44.88 ± 0.04	< 44.99	< 45.02	45.07 ± 0.04	14.48 ± 0.09	43.93 ± 0.04	1, 3, 7
PG1630+377	1.466	< 46.87	< 47.20	< 47.24	46.97 ± 0.04	...	44.97 ± 0.04	11, 3, 14
PG1634+706	1.334	47.15 ± 0.04	47.45 ± 0.04	47.49 ± 0.04	47.62 ± 0.04	...	45.71 ± 0.01	2, 3, 4
PG1700+518	0.292	46.08 ± 0.04	46.26 ± 0.04	46.30 ± 0.04	45.97 ± 0.04	14.50 ± 0.06	43.79 ± 0.04	1, 3, 10
PG2130+099	0.061	44.87 ± 0.04	45.00 ± 0.04	45.06 ± 0.04	44.81 ± 0.05	14.49 ± 0.05	43.57 ± 0.09	1, 12, 12
PG2302+029	1.044	< 46.74	< 47.13	< 47.20	47.16 ± 0.04	...	44.90 ± 0.04	11, 3, 14
Q0054+144	0.171	45.47 ± 0.03	45.57 ± 0.04	45.63 ± 0.04	45.24 ± 0.03	...	44.24 ± 0.08	11, 12, 5
Q0121–590	0.046	44.98 ± 0.04	45.06 ± 0.04	45.09 ± 0.04	45.04 ± 0.16	...	43.77 ± 0.13	11, 12, 12
Mrk205	0.071	44.72 ± 0.04	< 44.79	< 44.88	$44.56^{+0.17}_{-0.14}$...	43.92 ± 0.15	11, 11, 5
Mrk509	0.034	44.78 ± 0.04	44.89 ± 0.04	44.93 ± 0.04	44.69 ± 0.04	14.50 ± 0.11	44.61 ± 0.04	11, 11, 6
Mrk586	0.155	45.23 ± 0.03	45.48 ± 0.04	45.55 ± 0.04	45.33 ± 0.03	14.41 ± 0.14	44.01 ± 0.04	12, 12, 8
Mrk704	0.029	44.49 ± 0.06	< 44.61	< 44.64	44.12 ± 0.08	...	42.89 ± 0.04	11, 12, 10
Mrk705	0.029	44.24 ± 0.04	44.35 ± 0.04	44.40 ± 0.04	$43.92^{+0.16}_{-0.10}$...	43.18 ± 0.04	11, 12, 10
MR2251–178	0.064	44.80 ± 0.04	44.91 ± 0.04	< 44.95	44.98 ± 0.09	...	44.61 ± 0.04	11, 12, 5
PG1121+422	0.234	< 45.55	< 45.72	< 45.76	45.23 ± 0.04	14.49 ± 0.08	...	11, 13
PG1519+226	0.137	< 45.13	< 45.24	< 45.28	45.09 ± 0.04	14.53 ± 0.07	...	1, 3

Note. — (1): source name;(2): redshift; (3): infrared luminosity in $\text{erg s}^{-1}(1-25 \mu\text{m})$; (4): optical and ultraviolet luminosity in $\text{erg s}^{-1}(0.1-1\mu\text{m})$; (5): ratio between L_{IR} and L_{OUV} ; (6): spectral index; (9): dip frequency in Hz; (10): 2-10keV X-ray luminosity in erg s^{-1} ; (11): references (IR,OUV,HX).

APERTURES: *ISO* (μm): 4.8 (23''); 7.3, 12.0, 25 (52''); 60, 100 (45''). *IRAS* (μm): 10.1 (4.5''); 1.3–3.7 (5.5''). 1.0–0.01 (15'') in Neugbauer et al. (1987).

References. — 1: Haas et al. (2003); 2: Haas et al. (2000); 3: Neugbauer et al. (1987); 4: George et al. (2000); 5: Reeves et al. (2000); 6: Page et al. (2004); 7: Porquet et al. (2004); 8: Ueda et al. (2001); 9: Lawson et al. (1997); 10: the Tartarus Database; 11: NED; 12: Elvis et al. (1994); 13: Wilkes et al. (1999); 14: Piconcelli et al. (2004).